Optimization of electro-Fenton oxidation of biologically pretreated coal gasification wastewater by response surface methodology

Baolin Hou*, Wencheng Ma, Hongjun Han, Peng Xu, Haifeng Zhuang, Shengyong Jia, Kun Li

State Key Laboratory of Urban Water Resource and Environment, Harbin Institute of Technology, Harbin 150090, China, Tel. +86 15104682842; email: hbl527@163.com (B. Hou), Tel. +86 13796163639; email: damahit@126.com (W. Ma), Tel. +86 451 87649777, +86 13946003379; email: han13946003379@163.com (H. Han), Tel. +86 18724615294; email: h3i3t0@126.com (P. Xu), Tel. +86 187045138656; email: hit2014_3@163.com (H. Zhuang), Tel. +86 18804511681; email: jiashy06@sina.com (S. Jia), Tel. +86 13100809111; email: 913628173@qq.com (K. Li)

ABSTRACT

The response surface methodology coupled with central composite design was applied to optimize the operational parameters of electro-Fenton (EF) as advanced treatment of biologically pretreated coal gasification wastewater. The integration of TOC, COD, and total phenols removal was selected as the response for model establishment and optimization. A quadratic model with high significance was developed to predict the treatment performance and optimize process parameters. The optimal parameters were determined as pH 3.83, 1.44 mmol L^{-1} of Fe^{2+} concentration, and 16.28 mA cm^{-2} of current density, with the predicted optimal integration removal efficiency of 73.29%. TOC decay in the EF under optimal condition followed pseudo-first-order kinetic reaction with the apparent rate constant of 0.0103 min^{-1}. The mass transfer constant was determined to be 4.29×10^{-5} m s^{-1} at the optimal current density. The results demonstrated that EF could serve as a technically feasible and cost-effective method with potential applications for the advanced treatment of biologically stabilized coal gasification wastewater.

Keywords: Electro-Fenton; Response surface methodology; Central composite design; Coal gasification wastewater

1. Introduction

Coal gasification wastewater (CGW) generated from the coal chemical industry plant is a complex industrial wastewater with poor biodegradability. Environmental pollution by CGW sets a severe ecological problem, which is increased by the fact that most of them are difficult to be degraded using conventional treatment options. Conventional treatment of CGW includes a series of biological treatment after a physical–chemical pretreatment to reduce the concentrations of phenols and ammonium due to the low cost and maximal mineralization of pollutants [1,2]. However, the effectiveness of the traditional treatment system is unsatisfactory due to the presence of considerable amounts of recalcitrant and toxic compounds such as ammonia, cyanide, phenols, nitrogen heterocyclic compounds, polycyclic aromatic hydrocarbons,

*Corresponding author.

and other refractory contaminant. Among these toxic and recalcitrant compounds, phenols are the main pollutants in the wastewater [3]. Therefore, the biologically pretreated CGW still contains a large number of toxic and refractory compounds as well as their derivatives, with lower biodegradability than the raw wastewater, resulting in the failure to meet current strict effluent discharge standards [4,5].

Recently, advanced oxidation processes (AOPs) can be considered as potentially powerful methods and have been given growing interests in the post-treatment of industrial wastewater, aiming at the removal of the hard-to-biodegrade organics residual in the wastewater. As one of the AOPs, electro-Fenton (EF) has received great attention for water remediation because it can generate large amounts of oxidant hydroxyl radical ($\cdot$OH) for an effective and fast mineralization of toxic organic pollutants to CO_2, water, and inorganic ions [6,7]. Since OH production does not involve usage of the harmful chemicals which can be hazardous for the environment, this process is environmentally friendly for wastewater treatment and seems to be promising for the purification of water. The electrochemical production of H_2O_2 and regeneration of Fe^{2+} involved in EF avoid the addition of H_2O_2 and reduce the generation of ferrous sludge [8]. EF oxidation provides certain advantages for the removal of recalcitrant pollutants as well as some inorganic pollutants from the wastewater in cases where the requirement of the effluent quality is beyond the capacity of traditional processes [9]. In the EF system, O_2 or air gas is injected into either the reaction medium or directly at the cathode to generate H_2O_2 via reaction (1):

$$O_{2(g)} + 2H^+ + 2e^- \rightarrow H_2O_2 \qquad (1)$$
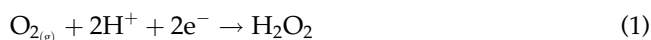
The cathodes that produce H_2O_2 efficiently are mainly carbonaceous electrodes such as activated carbon fiber [10], carbon felt [11,12], carbon–polytetrafluoroethylene (PTFE) [7,13], carbon nanotubes PTFE [14,15], and boron-doped diamond (BDD) [16]. The oxidizing power of electrogenerated H_2O_2 is enhanced by adding small amounts of Fe^{2+} to form Fe^{3+} and $\cdot$OH in the bulk via Fenton reaction (2). These radicals react with organic pollutants and thus lead to their oxidative degradation by hydrogen atom abstraction reaction, electron transfer, or electrophilic addition to p systems.

$$Fe^{2+} + H_2O_2 + H^+ \rightarrow Fe^{3+} + {}_\bullet OH + H_2O \qquad (2)$$

$$Fe^{3+} + e^- \rightarrow Fe^{2+} \qquad (3)$$
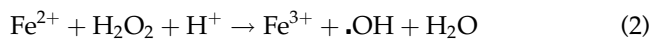
Reaction (2) is catalytic because it is primordially propagated from Fe^{2+} regeneration by Fe^{3+} reduction at the cathode (reaction (3)) [6]. When a one-compartment electrochemical reactor is employed, organic compounds can also be degraded by adsorbed hydroxyl radical (M($\cdot$OH)) that is formed as intermediate of water discharge at the anode M by reaction (4) [17]:

$$M + zH_2O - ze^- \rightarrow M({}_\bullet OH)_z + zH^+ \qquad (4)$$
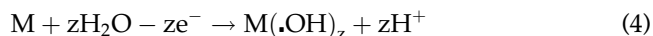
The BDD anode is preferred to produce absorbed hydroxyl radical since it generates BDD($\cdot$OH) radicals with greater oxidation power than those of other anodes like Pt and PbO_2 as a result of its higher oxygen overpotential [18,19]. However, the Pt anode producing less potent Pt($\cdot$OH) radicals is widely employed because it yields lower cost treatments by the lower potential difference applied to the cell [19,20].

The process parameters determine the performance. Many studies have exploited the probability of optimizing and predicting the results applying models based on reaction kinetics [21–23], artificial neural networks [24,25], and response surface methodology (RSM) [26]. Among these methods, RSM is a statistical-based method with wide application for designing experiments, evaluating the individual, and interaction effects of independent variables simultaneously, and optimizing the process parameters with limited number of trials according to special experimental design based on factorial designs [27,28]. Recently, this methodology has been applied to the optimization of several AOPs [15,29–31]. The application of RSM has demonstrated that this modeling can effectively optimize and predict the Fenton processes [24,32,33].

The objective of this study was to optimize the process parameters and investigate the application of EF in the advanced treatment of biologically stabilized CGW. A central composite design (CCD) using RSM was employed to assess the effects of the key experimental variables. The integration of TOC, COD, and total phenols removal was selected as the response for optimization and developing the quadratic model with the experimental data. The significance of each variable on the treatment performance was assessed and the optimal parameters were obtained and validated. The current efficiency and TOC degradation kinetics were inspected to evaluate the EF technology as advanced treatment of biologically stabilized CGW, comprehensively.

2. Experimental

2.1. Wastewater characteristics

Real CGW used in this study was collected from the effluent of a full-scale wastewater treatment facility of a coal gasification plant setup with anaerobic–anoxic–oxic (A–A–O) process, Harbin in China. The qualities of the biologically treated CGW were as follows: COD, 163.3 ± 14.1 mg L^{-1}; TOC, 43.6 ± 4.2 mg L^{-1}; BOD$_5$, 14.6 ± 4.1 mg L^{-1}, NH$_3$-N, 6.6 ± 1.8 mg L^{-1}; TN, 29.4 ± 2.6 mg L^{-1}; total phenols 48.3 ± 3.3 mg L^{-1}; and pH, 6.3–7.0. The effluent is much recalcitrant for further biological treatment (BOD$_5$/COD < 0.09).

2.2. Experimental design and fundamental and principles of RSM

It is common that the response variable Y (output variable) exists with a set of predictor variables x_1, x_2,..., x_k (input variables). In some cases, the underlying relationship between Y and the x might not be fully understood. Then an empirical model $Y = f(x_1, x_2,..., x_k) + \varepsilon$ is used to express the ambiguous relationship, where ε is the random error in the model, and f represents the unknown response surface. Generally, a first-order or second-order polynomial is deduced to describe the special f. This empirical model is called response surface model and the approximation of the response function $Y = f(x_1, x_2,..., x_k) + \varepsilon$ is called RSM.

In order to develop the proper approximation for f, either first order or second order polynomial models are employed.

In general, the first order model can be expressed as:

$$\begin{cases} Y = \beta_0 + B_1 X + \varepsilon = \beta_0 + \sum_{j=1}^{k} \beta_j x_j + \varepsilon \\ B_1 = [\beta_1 \beta_2 \cdots \beta_k] \end{cases} \quad (5)$$

And the second order model is

where B_1 and B_2 are the first and second order regression coefficient matrices, respectively, k is the number of independent variables, and β_0 is the constant coefficient. The second-order model describes a curving surface, including all terms in the first-order model, plus all quadratic terms and all interaction terms. The second order model was also called quadratic model.

Experimental design statistical analysis of the response surfaces were generated by the software design expert. The CCD consists of eight factorial points, six axial points, and six central points, constituting 20 trials. Six replicates in the central point were made to estimate the pure error. All the trials were randomly performed to minimize the effect of unexplained variability on the observed responses due to systematic errors. The levels of the variables used in the experiments were summarized in Table 1. The levels employed in the trials were determined according to the results of a previous orthogonal test.

The polynomial models developed were statistically validated by means of analysis of variance (ANOVA), checking the statistical significances from the F-test and fit quality from the squared correlation coefficients (R^2). The interaction effect between the variables was illustrated by the 3-D surface and 2-D contour plots. The optimal process parameters were calculated using the fitted models and validated by the experiments.

2.3. Experiment and analytical procedures

Trials were performed in a one-compartment electrochemical cell. The anode was a Pt sheet (4 cm × 5 cm × 0.3 cm) and the cathode was a piece of active carbon fiber (ACF) with the same dimension, both electrodes were fixed on two plastic brackets with the distance between the electrodes of 4 cm. The EF process was conducted in galvanostatic mode. Direct current was provided by DC stabilized power

$$Y = \beta_0 + B_1 X + X B_2 X + \varepsilon = \beta_0 + \sum_{j=1}^{k} \beta_j x_j + \sum_{j=1}^{k} \beta_{jj} x_j^2 + \sum_{j=1}^{k} \sum_{i=1}^{i<j} \beta_{ij} x_i x_j + \varepsilon$$

$$B_1 = [\beta_1 \quad \beta_2 \quad \cdots \quad \beta_k], \quad B_2 = \begin{bmatrix} \beta_{11} & \frac{1}{2}\beta_{12} & \cdots & \frac{1}{2}\beta_{1k} \\ \frac{1}{2}\beta_{21} & \beta_{22} & \cdots & \frac{1}{2}\beta_{2k} \\ \vdots & & \ddots & \vdots \\ \frac{1}{2}\beta_{k1} & \frac{1}{2}\beta_{k2} & \cdots & \beta_{kk} \end{bmatrix} \quad (6)$$

Table 1
Coded levels and real values for CCD and RSM analysis

Trial	Coded levels			Real values[a]			Removal efficiency (%)			
	x_1	x_2	x_3	X_1	X_2	X_3	TOC	COD	Total phenols	Integration
1	−1	−1	−1	3	1	15	49.89	61.87	72.16	61.3
2	1	−1	−1	4	1	15	54.14	65.76	77.88	65.92
3	−1	1	−1	3	2	15	49.26	61.14	72.34	60.91
4	1	1	−1	4	2	15	51.8	63.07	74.67	63.18
5	−1	−1	1	3	1	20	44.7	55.91	65.25	55.28
6	1	−1	1	4	1	20	48.89	59.72	70.87	59.82
7	−1	1	1	3	2	20	53.19	65.66	76.56	65.13
8	1	1	1	4	2	20	55.46	67.27	79.58	67.43
9	−1.68	0	0	2.66	1.5	17.5	49.12	60.98	71.41	60.5
10	1.68	0	0	4.34	1.5	17.5	53.27	65.76	77.78	65.6
11	0	−1.68	0	3.5	0.66	17.5	47.4	59.01	68.9	58.43
12	0	1.68	0	3.5	2.34	17.5	48.75	59.56	70.58	59.63
13	0	0	−1.68	3.5	1.5	13.3	52.18	64.72	75.57	64.15
14	0	0	1.68	3.5	1.5	21.7	49.39	60.29	71.43	60.37
15	0	0	0	3.5	1.5	17.5	60.19	73.51	85.78	73.16
16	0	0	0	3.5	1.5	17.5	59.97	72.76	85.9	72.87
17	0	0	0	3.5	1.5	17.5	59.83	72.81	84.98	72.54
18	0	0	0	3.5	1.5	17.5	60.42	73.55	86.48	73.48
19	0	0	0	3.5	1.5	17.5	60.79	73.81	86.22	73.6
20	0	0	0	3.5	1.5	17.5	59.66	72.94	85.6	72.73

[a]X_1. pH; X_2. Concentration of Fe^{2+} (mmol L^{-1}); X_3. Current density (mA cm^{-2}).

supply (WWL-PS) and the voltage and current could be accurately regulated and measured. Air was introduced and dispersed at the bottom of the ACF to provide oxygen for reaction (1) to continuously produce H_2O_2 and generate stirring in the solution. The initial pH was adjusted to the defined values by adding NaOH and H_2SO_4 solution and monitored using pHC101 probe equipped to a multifunction meter (HACH, USA). Desired quantity of granular ferrous sulfate ($FeSO_4·7H_2O$) was added into the solution followed by the adjustment of pH. Then the DC power was switched on to initiate the reaction. After defined reaction time, the power was switched off and the solution pH was adjusted to 8.5 to quench the reaction and precipitate the ferric ion. Then samples were taken into 50℃ water bath for 30 min to get rid of the unreacted H_2O_2, followed by filtration with 0.45 μm filter paper. Finally, samples were stored at 4℃ for further analysis. All the experiments were performed in triplicate, and the results were the average of at least three measurements with an accuracy of ±5%. The mineralization of biologically stabilized CGW was monitored from the TOC decay, measured with TOC analyzer (TOC-CPN, Shimadzu, Japan). COD and total phenols were determined according to standard methods. The current efficiency (CE) was estimated from Eq. (7).

$$CE = \frac{(TOC_{t_1} - TOC_{t_2})VF \times 4}{1000 \times 12I(t_2 - t_1)} \tag{7}$$

where F is the Faraday constant (96,485.34 C mol^{-1}), $(t_2 - t_1)$ is the electrolysis time (s), ($TOC_{t1} - TOC_{t2}$) is the environmental TOC decay (mg L^{-1}), V is the solution volume (L), I is the current (A), 4 is the number of electrons transferred per each TOC molecule, 1,000 is the conversion factor to homogenize units, and 12 is the molecular weight of TOC (g mol^{-1}).

3. Results and discussion

3.1. Validation of the model

The full factorial CCD and the results of each trial were presented in Table 1.

According to the data listed in Table 1, a quadratic model was developed using the RSM. The analysis of the observed responses (integration removal efficiency) presented in Table 1 yielded the following adjusted quadratic model at 95% confidence level.

$$
\begin{aligned}
Y = &-261.68 + 96.3x_1 + 29.81x_2 + 16.1x_3 \\
&-12.78x_1^2 - 18.47x_2^2 - 0.56x_3^2 \\
&-2.3x_1x_2 - 0.005x_1x_3 + 2.06x_2x_3
\end{aligned} \tag{8}
$$

Table 2
ANOVA test for the regression model

Source of variations	Sum of squares	DF	MS	F-value	Probability (p)
Regression	647.959	9	71.995	40.447	<0.00001
Residual	17.801	10	1.780		
Lack of fit	13.747	5	2.749	3.391	0.1031
Pure error	4.054	5	0.811		
Total	665.760	19			

The F-test from ANOVA was used to statistically validate the significance of regressions (Table 2). The F-value calculated for the regression of the model was 40.447, greater than 4.95 theoretically calculated for 99% confidence level, corroborating that the developed model was statistically significant. The F-value calculated for the lack of fit was 3.391, lower than 5.05 tabulated for 95% confidence level, indicating that it was satisfactory without evidencing a lack of fit. The F-test of the regression models produced very low p-value (<0.00001), suggesting high significance of the model. The squared correlation coefficient ($R^2 = 0.9733$) also confirmed the high precision and reliability of the trials. The residuals were randomly distributed around the mean in front of predicted values (Fig.1(a)), thereby discarding systematic errors. The predicted data were in good agreement with the observed data (Fig. 1(b)), evidencing the excellent description of EF by the quadratic model developed by RSM. The results also demonstrated that the developed regression model was competent to predict the response accurately.
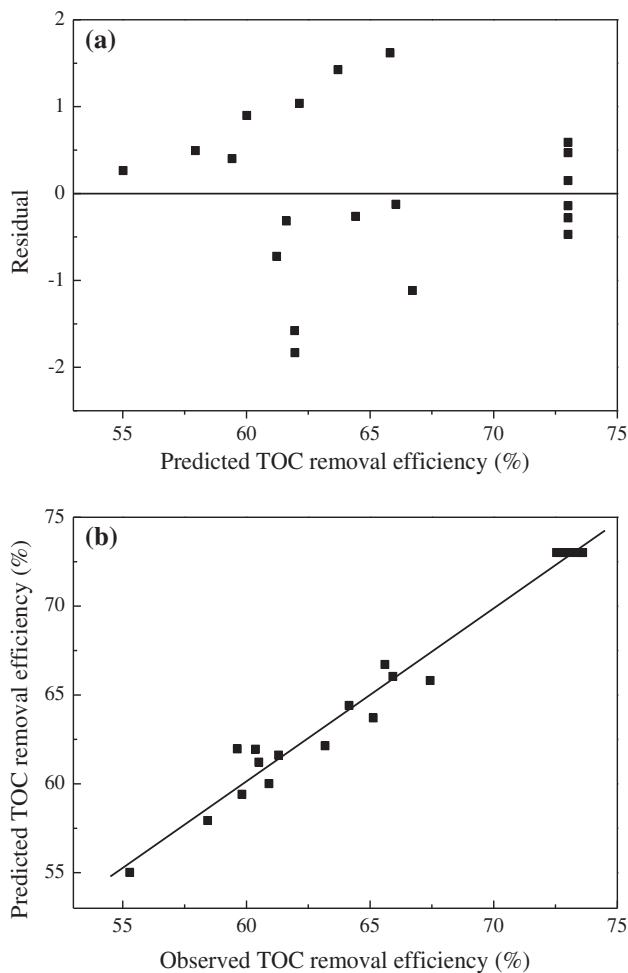
Fig. 1. (a) Residual vs. predicted and (b) predicted vs. observed values of TOC removal efficiency.

3.2. Influence of independent variables on the EF and the optimization

The 3-D response surface and 2-D contour plots of the integration removal efficiency regarding the interaction effects between independent variables were illustrated in Fig. 2. All the linear, quadratic, and interaction effects were significant except the interaction effect between pH and current density (x_1x_3). An optimal pH was observed in the response surfaces. Both lower and exceeding high pH exerted negative contribution to organics removal. Exceeding high pH reduced the reactive Fe^{2+} since pH affects the ferrous species. At the optimal pH, $Fe(OH)_2$ is the dominant ferrous form and is more reactive than Fe^{2+} in the catalysis of Fenton reaction. Low current efficiency under extreme acidic solution also restricted treatment performance since the progressive generation of $H_3O_2^+$ at lower pH makes H_2O_2 more electrophilic from reaction (9). Current is the power to generate H_2O_2. The rise in current density promoted the treatment performance, accounted for the generation of more amounts of H_2O_2 and hydroxyl radicals (·OH). While exceeding high current density presented negative effect on pollutant removal probably due to the loss of reactive (·OH) by the enhancement of its
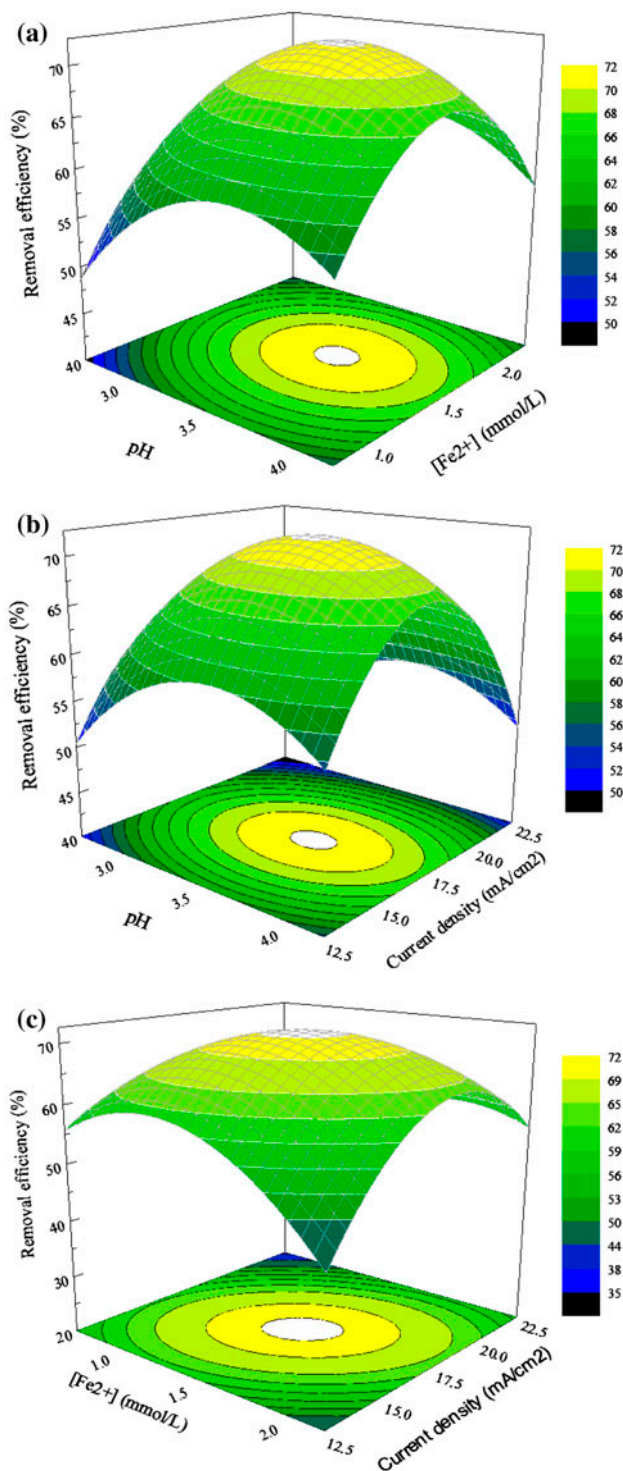
Fig. 2. Comparative response surfaces generated from RSM and 2-D contour plots of the integration removal efficiency illustrating the effect of two independent variables.

non-oxidizing reaction involvingfrom reaction (10). The oxidizing power of hydroperoxyl radical ($HO_2\cdot$) is weaker than that of ($\cdot OH$).

$$H_2O_2 + H^+ \rightarrow H_3O_2^+ \qquad (9)$$

$$H_2O_2 + \cdot OH \rightarrow HO_2^\cdot + H_2O \qquad (10)$$

Integration removal efficiency was high when adequate amount of Fe^{2+} was added since it is the catalyzer in the Fenton reaction. Treatment performance worsen with excess addition of Fe^{2+}, which is related to the rapid attack on $\cdot OH$ from reaction (11), causing the consumption of ($\cdot OH$), hence inhibiting the reaction with organics.

$$Fe^{2+} + \cdot OH \rightarrow Fe^{3+} + OH^- \qquad (11)$$

The interaction effect between Fe^{2+} concentration and current density was notable significance since both Fe^{2+} and electrogenetrated H_2O_2 are the main Fenton reagents. The increase in both current density and Fe^{2+} concentration boosts the Fenton reaction, promoting the mineralization process accordingly. The interaction effect between pH and current density was little significant owing to no relation between them in the EF. The interaction effect between pH and Fe^{2+} was not very significant, which may be explained by that the range of pH used in this study was close to the optimal value. According to the developed quadratic model and the response surface, the optimal parameters and predicted response under optimal conditions were listed in Table 3. The trial with optimal parameters was done as cross validation.

The removal efficiencies of TOC, COD, and total phenols under optimal condition were up to 60.41, 73.32, and 85.82%, respectively. When four pairs of electrodes were employed in this treatment system, power consumption per ton wastewater was 0.7 kWh with the effluent TOC, COD, and total phenols concentrations of 17.26, 43.56, and 6.84 mg L^{-1}. The overall organics removal efficiency highlighted the outstanding mineralization power of the EF process. The results demonstrated that EF could serve as a technically feasible and cost-effective method with potential applications for the advanced treatment of biologically stabilized CGW.

3.3. Decay kinetics for TOC removal

A quick decay of TOC was observed in the EF process under optimized condition (Fig. 3). The inset panel of Fig. 3 illustrated the excellent fitting of the above concentration decay with a pseudo-first-order kinetic equation. The apparent rate constant was determined as 0.0103 min^{-1}. The exponential decrease of TOC evidenced that its oxidative degradation by

Table 3
The optimal parameters predicted by RSM

pH	[Fe^{2+}] (mmol L^{-1})	Current density (mA cm^{-2})	Predicted integration removal efficiency (%)	Integration removal efficiency (%)	Current efficiency (%)[a]
3.83	1.44	16.28	73.29	73.18	36.49

[a]Current efficiency based on TOC removal.
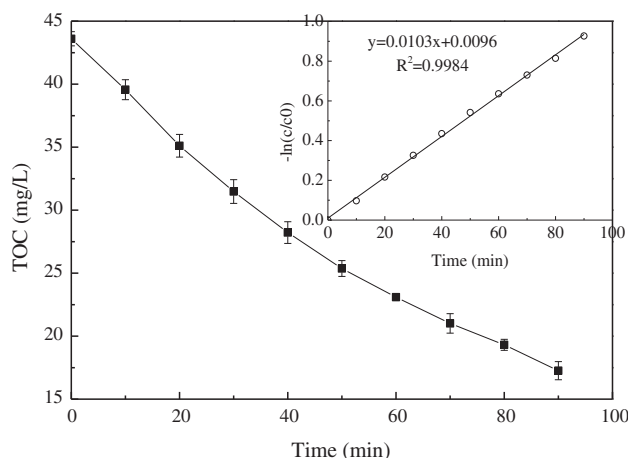
Fig. 3. TOC profile and kinetic fitting in the EF process.

(·OH) followed a pseudo-first-order reaction kinetic. Similar results have been reported for the reaction of hydroxyl radicals with organic compounds [34–36]. The obtained results were consistent with the previous literatures. It has been revealed that if the applied current density is greater than the limiting current density, the electrolysis is mass-transfer controlled and side reactions (such as oxygen evolution) may be involved [37]. The TOC decay kinetic within this range can be expressed by:

$$\frac{dTOC}{dt} = \frac{Ak_m}{V} TOC_{(t)} \qquad (12)$$

where k_m is the mass transfer constant (m s^{-1}), A is the area of the electrode (m^2). The mass transfer constant was 4.29×10^{-5} m s^{-1}, calculated from Eq. (12) and kinetic fitting (Fig. 3).

4. Conclusions

Biologically stabilized CGW was treated by the EF oxidation. A quadratic model with high significance was developed from the application of RSM coupled with CCD. The optimal parameters were obtained according to the optimization of the quadratic model. The model was competent to predict the response. The importance of interaction effects were revealed by the RSM model, which may be ignored by conventional experimental design. In addition, it should be noted that the information on reaction mechanisms cannot be reflected from RSM modeling, which is beyond the capability of RSM. The TOC degradation followed pseudo-first-order kinetics in the EF process, with the apparent rate constant of 0.0103 min^{-1}. The mass transfer constant was determined to be 4.29×10^{-5} m s^{-1}. The results demonstrated that EF could serve as a technically feasible and cost-effective method with potential applications for the advanced treatment of biologically stabilized CGW.

References

[1] H.B. Li, H.B. Cao, Y.P. Li, Y. Zhang, H.R. Liu, Innovative biological process for treatment of coking wastewater, Environ. Eng. Sci. 27 (2010) 313–322.
[2] B.L. Hou, H.J. Han, S.Y. Jia, H.F. Zhuang, Q. Zhao, P. Xu, Effect of alkalinity on nitrite accumulation in treatment of coal chemical industry wastewater using moving bed biofilm reactor, J. Environ. Sci. China 26 (2014) 1014–1022.
[3] H.F. Zhuang, H.J. Han, S.Y. Jia, B.L. Hou, Q. Zhao, Advanced treatment of biologically pretreated coal gasification wastewater by a novel integration of heterogeneous catalytic ozonation and biological process, Bioresour. Technol. 166 (2014) 592–595.
[4] H.F. Zhuang, H.J. Han, S.Y. Jia, Q. Zhao, B.L. Hou, Advanced treatment of biologically pretreated coal gasification wastewater using a novel anoxic moving bed biofilm reactor (ANMBBR)-biological aerated filter (BAF) system, Bioresour. Technol. 157 (2014) 223–230.
[5] H.F. Zhuang, H.J. Han, B.L. Hou, S.Y. Jia, Q. Zhao, Heterogeneous catalytic ozonation of biologically pretreated Lurgi coal gasification wastewater using

sewage sludge based activated carbon supported manganese and ferric oxides as catalysts, Bioresour. Technol. 166 (2014) 178–186.

[6] E. Brillas, I. Sires, M.A. Oturan, Electro-Fenton process and related electrochemical technologies based on Fenton's reaction chemistry, Chem. Rev. 109 (2009) 6570–6631.

[7] S. Garcia-Segura, L.C. Almeida, N. Bocchi, E. Brillas, Solar photoelectro-Fenton degradation of the herbicide 4-chloro-2-methylphenoxyacetic acid optimized by response surface methodology, J. Hazard. Mater. 194 (2011) 109–118.

[8] P.V. Nidheesh, R. Gandhimathi, Removal of Rhodamine B from aqueous solution using graphite-graphite electro-Fenton system, Desalin. Water Treat. 52 (2014) 1872–1877.

[9] O.T. Can, COD removal from fruit-juice production wastewater by electrooxidation electrocoagulation and electro-Fenton processes, Desalin. Water Treat. 52 (2014) 65–73.

[10] A.M. Wang, J.H. Qu, H.J. Liu, J. Ru, Mineralization of an azo dye Acid Red 14 by photoelectro-Fenton process using an activated carbon fiber cathode, Appl. Catal. B - Environ. 84 (2008) 393–399.

[11] M.A. Oturan, M.C. Edelahi, N. Oturan, K. El kacemi, J.J. Aaron, Kinetics of oxidative degradation/mineralization pathways of the phenylurea herbicides diuron, monuron and fenuron in water during application of the electro-Fenton process, Appl. Catal. B. Environ. 97 (2010) 82–89.

[12] M. Panizza, M.A. Oturan, Degradation of Alizarin Red by electro-Fenton process using a graphite-felt cathode, Electrochim. Acta. 56 (2011) 7084–7087.

[13] R. Salazar, S. Garcia-Segura, M.S. Ureta-Zanartu, E. Brillas, Degradation of disperse azo dyes from waters by solar photoelectro-Fenton, Electrochim. Acta. 56 (2011) 6371–6379.

[14] M. Zarei, A. Niaei, D. Salari, A. Khataee, Application of response surface methodology for optimization of peroxi-coagulation of textile dye solution using carbon nanotube-PTFE cathode, J. Hazard. Mater. 173 (2010) 544–551.

[15] A.R. Khataee, M. Zarei, L. Moradkhannejhad, Application of response surface methodology for optimization of azo dye removal by oxalate catalyzed photoelectro-Fenton process using carbon nanotube-PTFE cathode, Desalination 258 (2010) 112–119.

[16] K. Cruz-Gonzalez, O. Torres-Lopez, A. Garcia-Leon, J.L. Guzman-Mar, L.H. Reyes, A. Hernandez-Ramirez, J.M. Peralta-Hernandez, Determination of optimum operating parameters for Acid Yellow 36 decolorization by electro-Fenton process using BDD cathode, Chem. Eng. J. 160 (2010) 199–206.

[17] C.A. Martinez-Huitle, E. Brillas, Electrochemical alternatives for drinking water disinfection, Angew Chem. Int. Edit. 47 (2008) 1998–2005.

[18] E. Brillas, S. Garcia-Segura, M. Skoumal, C. Arias, Electrochemical incineration of diclofenac in neutral aqueous medium by anodic oxidation using Pt and boron-doped diamond anodes, Chemosphere 79 (2010) 605–612.

[19] C. Flox, C. Arias, E. Brillas, A. Savall, K. Groenen-Serrano, Electrochemical incineration of cresols: A comparative study between PbO$_2$ and boron-doped diamond anodes, Chemosphere 74 (2009) 1340–1347.

[20] M. Hamza, R. Abdelhedi, E. Brillas, I. Sires, Comparative electrochemical degradation of the triphenylmethane dye Methyl Violet with boron-doped diamond and Pt anodes, J. Electroanal. Chem. 627 (2009) 41–50.

[21] P. Kralik, H. Kusic, N. Koprivanac, A.L. Bozic, Degradation of chlorinated hydrocarbons by UV/H$_2$O$_2$: The application of experimental design and kinetic modeling approach, Chem. Eng. J. 158 (2010) 154–166.

[22] C. Zaror, C. Segura, H. Mansilla, M.A. Mondaca, P. Gonzalez, Kinetic study of Imidacloprid removal by advanced oxidation based on photo-Fenton process, Environ. Technol. 31 (2010) 1411–1416.

[23] C.K. Duesterberg, T.D. Waite, process optimization of Fenton oxidation using kinetic modeling, Environ. Sci. Technol. 40 (2006) 4189–4195.

[24] M.B. Kasiri, H. Aleboyeh, A. Aleboyeh, Modeling and optimization of heterogeneous photo-Fenton process with response surface methodology and artificial neural networks, Environ. Sci. Technol. 42 (2008) 7970–7975.

[25] E.S. Elmolla, M. Chaudhuri, M.M. Eltoukhy, The use of artificial neural network (ANN) for modeling of COD removal from antibiotic aqueous solution by the Fenton process, J. Hazard. Mater. 179 (2010) 127–134.

[26] N. Marchitan, C. Cojocaru, A. Mereuta, G. Duca, I. Cretescu, M. Gonta, Modeling and optimization of tartaric acid reactive extraction from aqueous solutions: A comparison between response surface methodology and artificial neural network, Sep. Purif. Technol. 75 (2010) 273–285.

[27] L. Wei, H. Zhu, X.H. Mao, F.X. Gan, Electrochemical oxidation process combined with UV photolysis for the mineralization of nitrophenol in saline wastewater, Sep. Purif. Technol. 77 (2011) 18–25.

[28] J. Virkutyte, E. Rokhina, V. Jegatheesan, Optimisation of Electro-Fenton denitrification of a model wastewater using a response surface methodology, Bioresour. Technol. 101 (2010) 1440–1446.

[29] O. Rozas, D. Contreras, M.A. Mondaca, M. Perez-Moya, H.D. Mansilla, Experimental design of Fenton and photo-Fenton reactions for the treatment of ampicillin solutions, J. Hazard. Mater. 177 (2010) 1025–1030.

[30] A.K. Abdessalem, N. Oturan, N. Bellakhal, M. Dachraoui, M.A. Oturan, Experimental design methodology applied to electro-Fenton treatment for degradation of herbicide chlortoluron, Appl. Catal. B. Environ. 78 (2008) 334–341.

[31] B.K. Korbahti, M.A. Rauf, Determination of optimum operating conditions of carmine decoloration by UV/H$_2$O$_2$ using response surface methodology, J. Hazard. Mater. 161 (2009) 281–286.

[32] H.S. Li, S.Q. Zhou, Y.B. Sun, J.A. Lv, Application of response surface methodology to the advanced treatment of biologically stabilized landfill leachate using Fenton's reagent, Waste Manage. 30 (2010) 2122–2129.

[33] Y.Y. Wu, S.Q. Zhou, F.H. Qin, X.Y. Ye, K. Zheng, Modeling physical and oxidative removal properties of Fenton process for treatment of landfill leachate using response surface methodology (RSM), J. Hazard. Mater. 180 (2010) 456–465.

[34] E. Brillas, M.A. Banos, J.A. Garrido, Mineralization of herbicide 3,6-dichloro-2-methoxybenzoic acid in aqueous medium by anodic oxidation, electro-Fenton and photo-electro-Fenton, Electrochim. Acta. 48 (2003) 1697–1705.

[35] A. Ozcan, M.A. Oturan, N. Oturan, Y. Sahin, Removal of Acid Orange 7 from water by electrochemically generated Fenton's reagent, J. Hazard. Mater. 163 (2009) 1213–1220.

[36] A. Ozcan, N. Oturan, Y. Sahin, M.A. Oturan, Electro-Fenton treatment of aqueous Clopyralid solutions, Int. J. Environ. Anal. Chem. 90 (2010) 478–486.

[37] J. Iniesta, P.A. Michaud, M. Panizza, G. Cerisola, A. Aldaz, C. Comninellis, Electrochemical oxidation of phenol at boron-doped diamond electrode, Electrochim. Acta. 46 (2001) 3573–3578.